

Generative Deep Learning Framework for Inverse Design of Fuels

Kiran K. Yalamanchi,[†] Pinaki Pal,^{*,†} Balaji Mohan,^{‡,||} Abdullah S. AlRamadan,[¶]
Jihad A. Badra,[‡] and Yuanjiang Pei[§]

[†]*Transportation and Power Systems Division, Argonne National Laboratory, 9700 S Cass Avenue, Lemont, IL 60439, USA*

[‡]*Digital R&D Division, Research and Development Center, Saudi Aramco, Dhahran, Saudi Arabia*

[¶]*Transport Technologies Division, Research and Development Center, Saudi Aramco, Dhahran, Saudi Arabia*

[§]*Aramco Americas: Aramco Research Center–Detroit, Novi, MI, USA*

^{||}*Deceased August 18, 2025.*

E-mail: pal@anl.gov

Abstract

In the present work, a generative deep learning framework combining a Co-optimized Variational Autoencoder (Co-VAE) architecture with quantitative structure-property relationship (QSPR) techniques is developed to enable accelerated inverse design of fuels. The Co-VAE integrates a property prediction component coupled with the VAE latent space, enhancing molecular reconstruction and accurate estimation of Research Octane Number (RON) (chosen as the fuel property of interest). A subset of the GDB-13 database, enriched with a curated RON database, is used for model training. Hyperparameter tuning is further utilized to optimize the balance among reconstruction fidelity, chemical validity, and RON prediction. An independent regression model

is then used to refine RON prediction, while a differential evolution algorithm is employed to efficiently navigate the VAE latent space and identify promising fuel molecule candidates with high RON. This methodology addresses the limitations of traditional fuel screening approaches by capturing complex structure-property relationships within a comprehensive latent representation. The generative model can be adapted to different target properties, enabling systematic exploration of large chemical spaces relevant to fuel design applications. Furthermore, the demonstrated framework can be readily extended by incorporating additional synthesizability criteria to improve applicability and reliability for *de novo* design of new fuels.

Introduction

Advancements in automotive technology, combined with the enforcement of strict environmental regulations, have created a critical need for innovative fuels that enhance engine efficiency while minimizing emissions. Modern engines require fuels with high knock resistance and cleaner combustion characteristics to support advanced operational capabilities. Traditional methods of fuel development, which heavily rely on experimental trial and error and expert intuition, are not only time-consuming but also inadequate for exploring the vast chemical space of potential fuel molecules. Considering these challenges, data-driven approaches have recently gained prominence as powerful tools for accelerating the discovery and optimization of fuels.

Generative deep learning models have significantly transformed the exploration and design of new chemical structures, particularly in the pharmaceutical industry. Models such as Variational Autoencoders (VAEs), Generative Adversarial Networks (GANs), and Reinforcement Learning (RL) frameworks have demonstrated a remarkable ability to generate novel, drug-like molecules with desired properties.¹⁻⁴ Inspired by these successes, researchers have begun applying generative models to fuel molecular design. Liu *et al.*⁵ introduced a generative fuel design framework effective in low-data scenarios by employing multi-objective

imitation learning. This suggests that generative models can be tailored to address fuel design challenges where data on candidate molecule properties is scarce. Furthermore, Rittig *et al.*⁶ presented a graph-based generative modeling strategy integrated with optimization algorithms to design high-octane fuels. Their graph machine-learning framework successfully identified known high-octane compounds. It proposed new fuel candidates, highlighting the growing potential of generative AI in discovering fuel molecules that meet specific performance requirements. Furthermore, recent work⁷ has employed LSTM-based generative model fine-tuned with hill-climb optimization to generate novel fuel molecules specifically optimized for high-knock resistance, demonstrating how generative approaches can be tailored to produce molecules with targeted fuel properties. Kuzhagaliyeva *et al.*⁸ expanded this concept to fuel mixtures, utilizing AI to design fuel blends with optimal performance, further demonstrating the versatility of AI-driven design in the combustion field. Recently, Yalamanchi *et al.*⁹ further enhanced this model by incorporating an uncertainty quantification (UQ) framework.

Simultaneously, significant progress has been made in machine learning-based Quantitative Structure-Property Relationship (QSPR) models for predicting fuel properties. Traditional QSPR methods often employ group contribution techniques or physicochemical descriptors to estimate metrics such as octane numbers. In recent years, data-driven models using molecular fingerprints and graph representations have achieved improved accuracy in predicting octane numbers and sensitivities. Vom Lehn *et al.*¹⁰ showed that tailoring feature sets for specific targets—such as Research Octane Number (RON) and Motor Octane Number (MON)—and selecting appropriate machine learning algorithms, including neural networks, enhanced predictive performance for gasoline compounds. SubLaban *et al.*¹¹ developed artificial neural network models for RON and octane sensitivity, providing a QSPR approach for fuel design. Their models underscored the effectiveness of nonlinear machine learning in capturing complex structure-property relationships beyond the capabilities of linear correlations. Additionally, Mohan and Chang¹² introduced an automated machine

learning framework called ChemSL, which evaluates multiple algorithms and hyperparameters to construct robust models for property prediction. Such automated and optimized approaches are particularly relevant when integrated with generative models, ensuring the predictive component maintains high accuracy. Chen *et al.*¹³ demonstrated a comprehensive approach of screening millions of fuel candidates using QSPR models to identify molecules tailor-made for specific applications, highlighting how these predictive models can be used to evaluate the practical application potential of vast molecular libraries. However, these QSPR-based approaches differ fundamentally from generative methods by focusing on property prediction and screening rather than molecular generation. While QSPR models excel at evaluating properties of known or proposed structures, they do not inherently generate novel molecular candidates, highlighting a key methodological distinction from generative approaches that can explore uncharted regions of chemical space.

These studies suggest that generative models, such as VAEs, can learn meaningful molecular representations that are useful for proposing new fuel molecules, and machine learning-based QSPR models can accurately predict key fuel properties when properly tuned. However, while advanced machine learning methods can enhance prediction accuracy, many QSPR models are trained on relatively limited datasets with hand-crafted features, which may not generalize across broad chemical spaces. This limitation introduces the risk of overlooking promising novel compounds outside the model’s experience. There is a growing interest in integrating generative and predictive modeling for fuel design to overcome these challenges. Researchers can efficiently navigate the chemical space to identify molecules with desired fuel properties by coupling a generative model with a property predictor. By training generative models on comprehensive chemical databases that cover a vast chemical space and applying property predictions to the latent representations or generated candidates, researchers can efficiently conduct targeted searches for molecules with desired properties. Liu *et al.*¹⁴ developed a VAE architecture that jointly optimized the compression objective and property prediction within a single integrated framework. This demonstrates the model’s

ability to capture essential chemical features relevant to predicting heating values and ignition metrics, even when property data were limited. These insights inform the approach adopted in this work, which builds on this concept by separating the generative and predictive components into distinct models. This modular design enhances flexibility, allowing independent training and optimization of the VAE-based generative model and the data-driven property predictor, ultimately improving the robustness and performance of each component.

The authors' previous work¹⁵ developed a VAE-based framework that learns a continuous latent representation of molecular structures suitable for generation and prediction. The VAE was trained on a downsampled GDB-13 chemical database using one-hot-encoded Simplified Molecular Input Line Entry System (SMILES) strings as input. Strategies to balance reconstruction fidelity and latent space regularization through the weightage of the regularization term (β) were systematically investigated. It was found that gradually increasing β to a moderate value (0.25) provided the best trade-off between reconstruction accuracy and latent space consistency. Higher β values risked posterior collapse—where the decoder ignores latent features—while lower β values led to poor regularization. Advanced techniques, such as cyclical β schedules,¹⁶ hierarchical priors,¹⁷ and penalizing latent variable correlations,¹⁸ were also explored. The results indicated that although a hierarchical latent prior offered some improvements in reconstruction accuracy, its benefits were modest, and substantial penalization of latent total correlation degraded performance. Employing a standard VAE with an annealed β schedule up to 0.25 captured most of the improvements.

Building upon these findings, the current study focuses on a streamlined yet enhanced VAE-based model for inverse fuel design. To this end, a co-optimized VAE (Co-VAE) approach is introduced that directly incorporates fuel property information into the generative model, aiming to steer the latent space toward meaningful features for property prediction. This Co-VAE is trained using the previously optimized β -annealing schedule, which increases β from zero to 0.25 over 75 epochs without introducing additional complexities, such as hi-

erarchical priors or total-correlation regularization. Concurrently, rigorous hyperparameter optimization (HPO) of the Co-VAE architecture and training process is performed using Bayesian optimization to ensure that the model’s capacity and learning dynamics are tuned to the data. Additionally, a QSPR modeling step is integrated by mapping the learned latent representations to the target fuel property (Research Octane Number - RON) constructing separate regression models for fine-tuning. Multiple machine learning algorithms are evaluated for this task, applying systematic hyperparameter searches to identify the optimal predictor. Subsequently, a latent space screening approach is used to pinpoint molecular candidates exhibiting promising fuel property. Combining the optimized predictive model with a robust global search strategy and thorough chemical validity checks, a diverse set of high-RON molecules are obtained for further investigation.

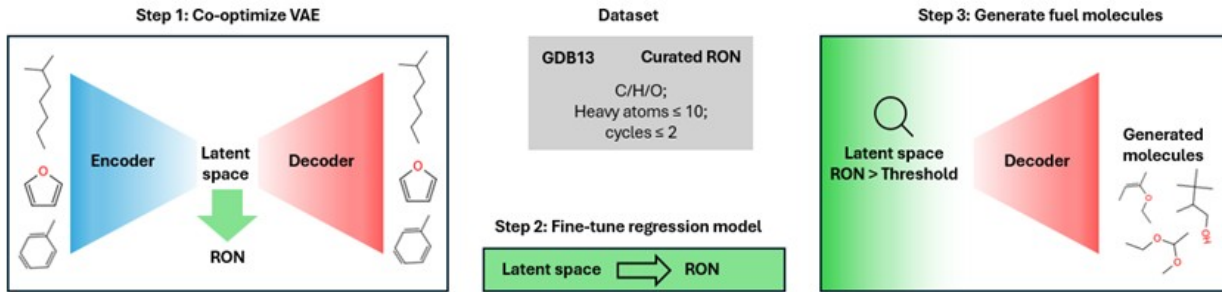


Figure 1: Integrated approach for generative fuel design. Step 1: Co-optimize the VAE for molecular reconstruction and RON prediction. Step 2: Fine-tune the regression model to enhance RON estimation. Step 3: Explore latent space regions linked to high RON and decode the corresponding species.

This integrated approach, shown in Figure 1, leverages the strengths of both generative and predictive models, facilitating an efficient exploration of the chemical space to design novel fuel molecules with desired properties. By combining a VAE-based generative model with a data-driven property predictor and employing advanced optimization techniques, we aim to maximize the effectiveness of each component in the workflow. The proposed methodology streamlines the fuel design process and addresses the limitations of traditional methods by harnessing the power of machine learning to navigate the vast chemical landscape.

Co-VAE Model Development

Data Curation and Processing

The datasets used in this study are fundamental to developing the Co-VAE model and accurately predicting RON. Building upon the authors' previous work,¹⁵ a refined subset of the GDB-13 database¹⁹ was employed, which is an extensive collection of small organic molecules containing up to 13 heavy atoms encompassing over 970 million unique compounds. The subset was downselected by focusing on molecules relevant to fuel applications, tailoring the dataset to the specific objective of fuel design, and managing computational feasibility. Specifically, compounds composed solely of carbon (C), hydrogen (H), and oxygen (O) atoms were selected, and the molecular size was limited to those containing up to 10 heavy atoms. This initial refinement yielded a dataset of 418,274 unique species, offering a manageable yet diverse representation of potential fuel molecules. In the present work, this dataset was further pruned by removing species containing more than two cyclic rings. Highly polycyclic compounds introduce significant structural complexity and are less pertinent to practical fuel formulations. This additional filtering ensures that the dataset remains focused on molecules that are both computationally tractable and relevant to fuel chemistry.

Experimental RON data was further integrated to enhance the dataset's applicability to property prediction tasks. A comprehensive RON dataset was curated from literature sources,^{8,20} which compile ASTM-compliant RON values, most of which originate from previously reported experimental measurements.²¹ This careful curation, applying the same down-sampling criteria as those used for the GDB-13 dataset, resulted in a dataset comprising 332 species along with associated RON values. Although the downselected GDB dataset is large, it is still not exhaustive of all fuel-like species and therefore missed out some species from the RON dataset. These missing species were incorporated into the dataset to ensure comprehensive coverage and maximize the model's ability to learn structure-property relationships. With this incorporation, the final downsized dataset comprises 357,907 species.

Molecular structures were represented using the SMILES notation, which encodes complex molecular graphs into linear strings suitable for computational processing. These SMILES strings were converted into one-hot encoded representations to serve as inputs to the Co-VAE model. The one-hot encoding process involved mapping each character in the SMILES string to a unique position in a binary vector, resulting in a fixed-length, two-dimensional array. All SMILES strings were padded to a maximum length of 23 characters to maintain consistency, and the character set comprised eight unique symbols representing atoms and molecular substructures.¹⁵ This encoding ensures that the input data is uniform in size and compatible with the Long Short-Term Memory (LSTM) networks employed in the Co-VAE architecture (discussed in the next subsection). Using one-hot encoding for SMILES strings facilitates the direct reconstruction of molecular structures from the latent space embeddings generated by the Co-VAE model. This approach offers advantages over traditional molecular descriptor-based methods by enabling an interpretable transformation between molecular structures and their encoded representations without requiring similarity search algorithms.

Model Architecture

The Co-VAE model developed in this study builds upon the authors' previous VAE framework, designed for molecular generation and property prediction. The original VAE architecture consists of a two-layer Long Short-Term Memory (LSTM) network,²² serving as the encoder, which is chosen for its ability to capture sequential dependencies in one-hot encoded SMILES strings that represent molecular structures. The encoder processes the input sequences and funnels the information through two fully connected (FC) layers into the latent space, producing means and log-variances that define the distribution from which latent variables are sampled. The decoder mirrors this structure in reverse, expanding the latent variables back to their original dimensionality through fully connected (FC) layers and reconstructing the input sequences using an LSTM network over the sequence length. For a

more detailed description of this architecture, the readers are referred to authors' previous work.¹⁵

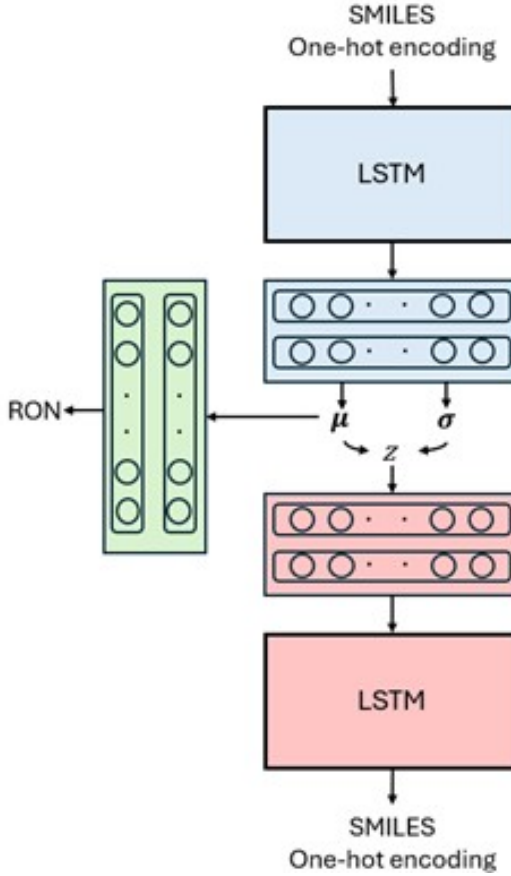


Figure 2: Co-VAE framework used in this study: an LSTM encoder translates SMILES one-hot encoding representation into a latent space, from which an LSTM decoder reconstructs the molecular one-hot encoding, while a feedforward network co-optimizes the latent space for RON prediction.

In the current study, the above architecture was extended by integrating a property prediction component into the generative model, aiming to steer the latent space toward features meaningful for predicting RON. Specifically, an additional feedforward neural network is introduced with two layers that connect from the means of the latent space to the RON prediction. The complete architecture of the Co-VAE model is shown in Figure 2. This modification lets the model learn informative latent representations for molecular reconstruction and property estimation. The Co-VAE training loss function is accordingly updated to include the RON prediction loss alongside the original reconstruction loss quantified by Binary

Cross-Entropy (BCE) and the Kullback-Leibler Divergence (KLD) regularization term. The overall loss function becomes:

$$\text{Loss} = \text{BCE} + \beta * \text{KLD} + L_{\text{RON}} \quad (1)$$

where β is the weight balancing the contribution of the KLD term. BCE quantifies the reconstruction error by measuring the cross-entropy between predicted and target binary values in the SMILES strings, while KLD regularizes the latent space by penalizing deviations from a standard normal distribution. L_{RON} represents the mean absolute error (MAE) associated with RON prediction.

The same optimal β -annealing schedule identified in the authors' previous work is maintained, gradually increasing β from zero to 0.25 over 75 epochs and maintaining it at 0.25 thereafter. This approach balances reconstruction fidelity and latent space regularization, thereby preventing issues such as posterior collapse, where the decoder ignores the latent variables. It is ensured that the model remains streamlined and effective by incorporating the RON prediction loss without altering the annealing schedule or introducing additional complexities, such as hierarchical priors or total correlation regularization.

Hyperparameter Optimization

Optimizing the hyperparameters of the Co-VAE model is crucial for enhancing its performance in both molecular generation and property prediction tasks. This study systematically explored various hyperparameters that influence the neural network's capacity, the complexity of the latent space, and the efficiency of the training process. The hyperparameters varied and included the number of layers in the LSTM encoder and decoder, the hidden size of the LSTM layers, the sizes of the fully connected and conditioning layers, the dimensionality of the latent space, and the batch size. The specific ranges within which these hyperparameters were varied are provided in Table 1. The learning rate remained fixed at 1×10^{-3} and

the number of training epochs was set to 300. Preliminary experiments indicated that the model consistently converged within this epoch range, justifying the fixed number of epochs and learning rate. The architecture’s capacity and latent space properties were optimized to fine-tune the model, enabling it to capture the essential features necessary for accurate molecular reconstruction and RON prediction.

Table 1: Hyperparameter ranges tested for the Co-VAE model.

Parameter	Value
Number of layers in LSTM	2 – 3
Hidden size of each LSTM layer	64 – 256
Fully Connected layer size	50 – 150
Conditioning layer size	10 – 100
Latent Space dimensionality	32 – 128
Batch size	64 – 256
Learning rate	10^{-3}
Number of epochs	300

The downselected GDB-13 dataset was split into 95% for training, 2.5% for validation, and 2.5% for testing. For the RON dataset, 10 species were selected for the validation set and 10 for the test set. To ensure statistical diversity, stratified sampling was employed based on molecular size and functional groups for the GDB-13 dataset, and based on molecular size for the RON dataset. The BCE and KLD terms in the loss function are computed for the entire GDB-derived dataset, regardless of whether or not RON measurements are available. However, only the molecules with experimentally measured RON values contribute to L_{RON} . Specifically, when a molecule in a training batch has a known RON value, its RON prediction error is included alongside the BCE and KLD loss terms; for other molecules, only the BCE and KLD loss terms are non-zero. To efficiently navigate the hyperparameter space, Bayesian optimization using the `bayes_opt` package²³ was employed. This methodology is well-suited for optimizing complex functions where evaluation is costly, as it intelligently selects hyperparameter configurations based on previous results to improve performance iteratively. The optimization process was initiated with 16 random evaluations to broadly explore diverse regions of the hyperparameter space. Following this initial exploration, sequential

optimization steps were conducted, selecting 8 points per batch and performing 40 runs. This approach enabled us to progressively refine the hyperparameters based on the observed model performance. The optimization metric was defined as a composite score based on the validation set, combining reconstruction accuracy, validity of generated molecules, and loss associated with predicting RON. Reconstruction accuracy measures the model’s ability to recreate input SMILES strings from the latent representations accurately. Validity assesses the proportion of generated molecules from the sampled normal distribution for latent space that is chemically plausible and adheres to established chemical valency rules, ensuring that outputs are meaningful within the domain of chemistry. Including the RON prediction loss in the metric encourages the latent space to be informative for property prediction, aligning the generative model with the target predictive task.

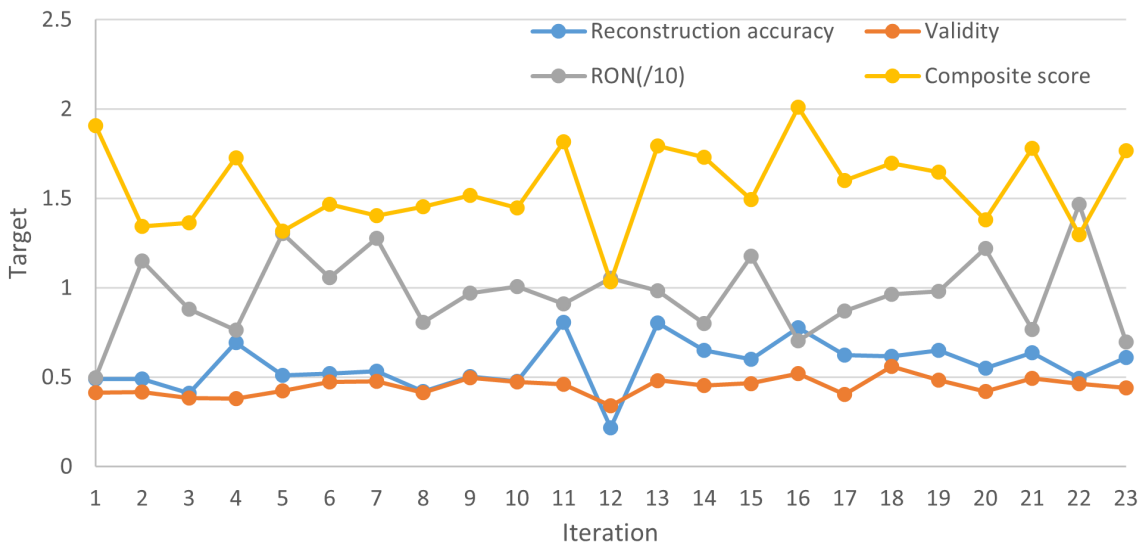


Figure 3: Reconstruction accuracy, validity, and RON MAE computed on validation set for the hyperparameter optimization iterations of Co-VAE. Composite score represents the sum of reconstruction accuracy, validity and five times the inverse of RON MAE.

The results of the HPO, derived from the validation set, are depicted in Figure 3, which illustrates the optimization metrics over iterations. Different configurations yielded varying performance levels across the optimization runs. The composite score is computed as the sum of reconstruction accuracy, validity and five times the inverse of RON MAE to ensure

comparable magnitudes. Upon completing the optimization runs, the hyperparameter configuration that yielded the best composite score on the validation set was selected as the optimal model, corresponding to iteration 16 in Figure 3. The specific values for each hyperparameter for this optimal configuration and the corresponding results on the test set are summarized in Table 2. The relatively high MAE of RON prediction from the Co-VAE model can be attributed to the significant difference in dataset sizes, with the RON dataset being orders of magnitude smaller than the downselected GDB-13 dataset. This limitation necessitates the development of a separate regression model, which will be discussed in the following section.

Table 2: Best hyperparameter combination obtained from HPO for the Co-VAE model and its performance on the test set.

Parameter	Value
Number of layers in LSTM	2
Hidden size of LSTM layer	151
Fully Connected Layer 1 size	84
Fully Connected Layer 2 size	72
Conditioning Layer 1 size	49
Conditioning Layer 2 size	19
Latent Space size	73
Batch size	172
Reconstruction accuracy	77.56%
Validity	55.19%
RON MAE	9.26

Regression Model Development for RON

To further enhance the accuracy of RON predictions, a separate regression model is developed using the latent space representations generated by the optimized Co-VAE model. By decoupling the fuel property prediction from the Co-VAE, a wider array of machine learning algorithms can be explored and rigorous HPO can be performed beyond the constraints of the feedforward neural network within the Co-VAE architecture. The RON dataset used for this regression task is consistent with the dataset described earlier for the Co-VAE model,

ensuring continuity in data usage. Specifically, the same training set from the Co-VAE model was used to develop the regression model. This training set was subjected to 10-fold cross-validation, a robust technique that assesses model performance across multiple data splits, reducing variance and mitigating overfitting. The remaining data from the dataset was employed as the test set for evaluating predictive capabilities of the regression model.

Leveraging the latent space embeddings from the Co-VAE model, various regression algorithms were explored to determine the most effective model for RON prediction. This approach enables us to leverage the rich, informative features captured in the latent space while tailoring the regression model to best fit the specific characteristics of the RON prediction task. The study investigated a range of model classes—including ensemble-based methods, linear regression techniques, regularization, deep learning (TabNet),^{24,25} and SuperLearner approaches^{12,26–28}—each of which offers unique advantages for capturing diverse patterns and relationships in the data. Comprehensive hyperparameter optimization was performed for each model using NSGA-2²⁹ from the Pymoo package.³⁰ This multi-objective evolutionary algorithm simultaneously optimized Coefficient of Determination (R^2), MAE, and Root Mean Squared Error (RMSE), ensuring a balanced trade-off between predictive accuracy and generalization. A population size of 100 and 20 iterations were employed during the NSGA-2 optimization, which was carried out over the complete hyperparameter search space (see Table 3) with 10-fold cross-validation to mitigate overfitting. The candidate with the minimum MAE value was selected as the best candidate from the Pareto front. The candidate selection is mathematically formulated as follows:

$$x^* = x_{\arg \min_i F_i^{(1)}} \quad (2)$$

Here, $F_i^{(1)}$ represents the MAE for the i^{th} candidate, and x^* denotes the optimal hyperparameter configuration corresponding to the minimum MAE value. Table 4 illustrates the performance of all evaluated models on the RON test set, where the CatBoost model emerged

Table 3: Regression models and hyperparameter ranges explored for RON prediction using latent space embeddings from the Co-VAE model.

Model	Hyperparameters
XGBoost	<code>n_estimators</code> [50, 1000], <code>max_depth</code> [1, 15], <code>learning_rate</code> [0.001, 0.3], <code>gamma</code> [0, 5], <code>min_child_weight</code> [1, 10], <code>subsample</code> [0.5, 1], <code>colsample_bytree</code> [0.5, 1], <code>reg_alpha</code> [0, 1], <code>reg_lambda</code> [0, 1]
CatBoost	<code>iterations</code> [50, 1000], <code>learning_rate</code> [0.001, 0.3], <code>depth</code> [1, 10], <code>l2_leaf_reg</code> [1, 10], <code>rsm</code> [0.5, 1], <code>bagging_temperature</code> [0, 1], <code>border_count</code> [32, 255]
LightGBM	<code>n_estimators</code> [50, 1000], <code>learning_rate</code> [0.001, 0.3], <code>num_leaves</code> [31, 256], <code>max_depth</code> [-1, 15], <code>min_child_samples</code> [5, 100], <code>subsample</code> [0.5, 1], <code>colsample_bytree</code> [0.5, 1], <code>reg_alpha</code> [0, 1], <code>reg_lambda</code> [0, 1], <code>min_split_gain</code> [0, 1]
RandomForest	<code>n_estimators</code> [50, 500], <code>max_depth</code> [3, 20], <code>min_samples_split</code> [2, 10], <code>min_samples_leaf</code> [1, 10], <code>max_features</code> [0.1, 1.0]
GradientBoosting	<code>n_estimators</code> [50, 500], <code>learning_rate</code> [0.01, 0.3], <code>max_depth</code> [3, 10], <code>min_samples_split</code> [2, 10], <code>min_samples_leaf</code> [1, 10], <code>subsample</code> [0.5, 1.0], <code>max_features</code> [0.5, 1.0]
LinearRegression	<code>fit_intercept</code> [0, 1], <code>copy_X</code> [0, 1]
Ridge	<code>alpha</code> [0.1, 100], <code>fit_intercept</code> [0, 1], <code>solver</code> {auto, svd, cholesky, lsqr, sparse_cg, sag, saga}, <code>max_iter</code> [100, 1000]
Lasso	<code>alpha</code> [0.0001, 1], <code>fit_intercept</code> [0, 1], <code>max_iter</code> [100, 1000], <code>selection</code> {cyclic, random}
ElasticNet	<code>alpha</code> [0.0001, 1], <code>l1_ratio</code> [0, 1], <code>fit_intercept</code> [0, 1], <code>max_iter</code> [100, 1000], <code>selection</code> {cyclic, random}
SVR	<code>C</code> [0.1, 100], <code>epsilon</code> [0.001, 1], <code>gamma</code> [0.0001, 1], <code>kernel</code> {linear, poly, rbf, sigmoid}, <code>degree</code> [2, 5]
KNeighbors	<code>n_neighbors</code> [1, 50], <code>weights</code> {uniform, distance}, <code>algorithm</code> {auto, ball_tree, kd_tree, brute}, <code>leaf_size</code> [10, 50], <code>p</code> [1, 2]
DecisionTree	<code>max_depth</code> [3, 20], <code>min_samples_split</code> [2, 20], <code>min_samples_leaf</code> [1, 20], <code>max_features</code> [0.1, 1.0], <code>splitter</code> {best, random}, <code>ccp_alpha</code> [0.0, 0.1]
TabNet	<code>n_d</code> [8, 64], <code>n_a</code> [8, 64], <code>n_steps</code> [3, 10], <code>gamma</code> [1.0, 2.0], <code>n_independent</code> [1, 5], <code>n_shared</code> [1, 5], <code>momentum</code> [0.01, 0.4], <code>lambda_sparse</code> [1e-4, 1e-2], <code>lr</code> [1e-3, 1e-1]

as the top performer for RON prediction based on latent space representations, achieving an R^2 of 0.929, an MAE of 5.365, and an RMSE of 8.090. This performance is on par with recent literature reporting MAE values of 5.22⁷ and 4.86,¹³ though Chen *et al.*¹³ work achieved 3.71 MAE by incorporating additional branching ratio feature, which could potentially be integrated into our framework for future improvements.

Table 4: Performance comparison of various regression models on RON test set.

Model	MAE	RMSE	R^2
CatBoost	5.365	8.090	0.929
XGBoost	6.513	10.496	0.880
LightGBM	6.959	10.556	0.878
AutoTS	7.130	10.640	0.875
TabNet	7.438	10.689	0.876
GradientBoosting	7.679	10.841	0.867
Lasso	7.679	11.034	0.859
LinearRegression	8.138	11.646	0.840
Ridge	8.574	12.106	0.852
ElasticNet	8.586	12.161	0.840
KNeighbors	8.684	12.896	0.818
DecisionTree	9.105	13.510	0.801
SVR	9.761	16.052	0.719
RandomForest	7.310	10.689	0.872

To further ensure the robustness of the final model, an additional 10-fold cross-validation was performed on the entire RON dataset using the CatBoost model, configured with the best hyperparameters obtained from the multi-objective optimization. The final optimized model demonstrated a cross-validation performance of $R^2 = 0.869 \pm 0.102$, MAE = 4.935 \pm 1.041, and RMSE = 7.879 \pm 2.964, as shown in the parity plot in Figure 4. The worst-performing outlier is n-propyl cyclohexane and exhibits a predicted RON value significantly higher than the experimental value. This optimized model is the basis for the subsequent molecular screening described in the next section. By integrating the latent space embeddings from the Co-VAE with advanced regression techniques, the RON prediction accuracy was effectively improved compared to the initial property predictor within the Co-VAE. This two-step approach—first learning a rich latent representation through the Co-VAE and then

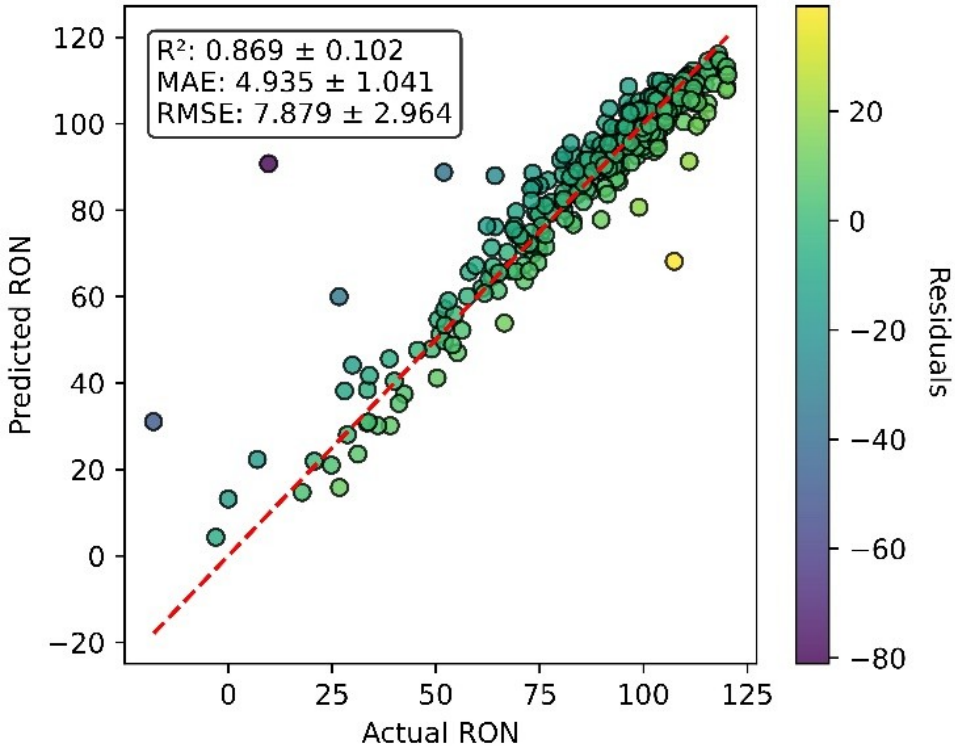


Figure 4: Parity plot for the final optimized CatBoost model. The ranges (error bars) shown for R^2 , MAE, and RMSE reflect the variability observed for the 10-fold cross-validation study.

fine-tuning a separate regression model—demonstrates the efficacy of combining deep generative models with traditional machine learning algorithms in the context of fuel property prediction. This methodology enhances the accuracy of property prediction and provides a flexible framework for exploring complex chemical spaces in fuel design. Decoupling the regression model allows for the inclusion of more sophisticated algorithms and optimization strategies, potentially leading to further improvements in predictive performance. Note that this does not necessarily mean the latent representation alone surpasses other feature formats or that CatBoost is universally superior to neural networks; rather, it illustrates how the Co-VAE’s generative capabilities, when paired with a diverse set of predictive models, can effectively facilitate targeted fuel design.

Generation of Promising High-RON Fuel Molecules

Building upon the optimized Co-VAE and regression model developed in the previous sections, the latent space was searched to identify novel fuel molecule candidates with high Research Octane Numbers (RON). The objective of this screening process is to generate molecular candidates with predicted RON values exceeding a certain threshold, which is set to 110, exploring the potential for advanced high-performance fuels. It was necessary to define appropriate boundaries for each latent dimension to explore this space for potential high-RON candidates systematically. The minimum and maximum values for each latent variable were computed across the entire combined RON dataset, which provided the natural limits of the latent space as learned by the model. To facilitate the exploration of regions just beyond the known data, which may contain novel and promising molecules, each latent variable's range was extended by 10% of its respective span. This expansion of the search space ensures that the optimization algorithm is not constrained strictly within the confines of the existing data distribution but is still guided by the learned latent structure of chemically relevant molecules.

To identify latent vectors corresponding to molecules with predicted RON values above 110, the Differential Evolution (DE) algorithm—a population-based, stochastic optimization method designed for continuous and high-dimensional spaces—is employed. DE utilizes mutation, crossover, and selection, inspired by natural evolution, to maximize the predicted RON from the regression model, subject to defined bounds of the latent space. The SciPy implementation of DE is leveraged to perform this optimization.³¹ Once high-predicted RON latent vectors were identified, they were decoded into molecular structures using the decoder component of the Co-VAE model, which transforms each latent vector into a sequence of tokens representing a SMILES string. The generated SMILES strings underwent a two-step validation process to ensure chemical feasibility and consistency in the predicted performance. First, the RDKit, an open-source cheminformatics library,³² was used to verify that each SMILES string adheres to chemical valency rules and proper syntax, discarding any

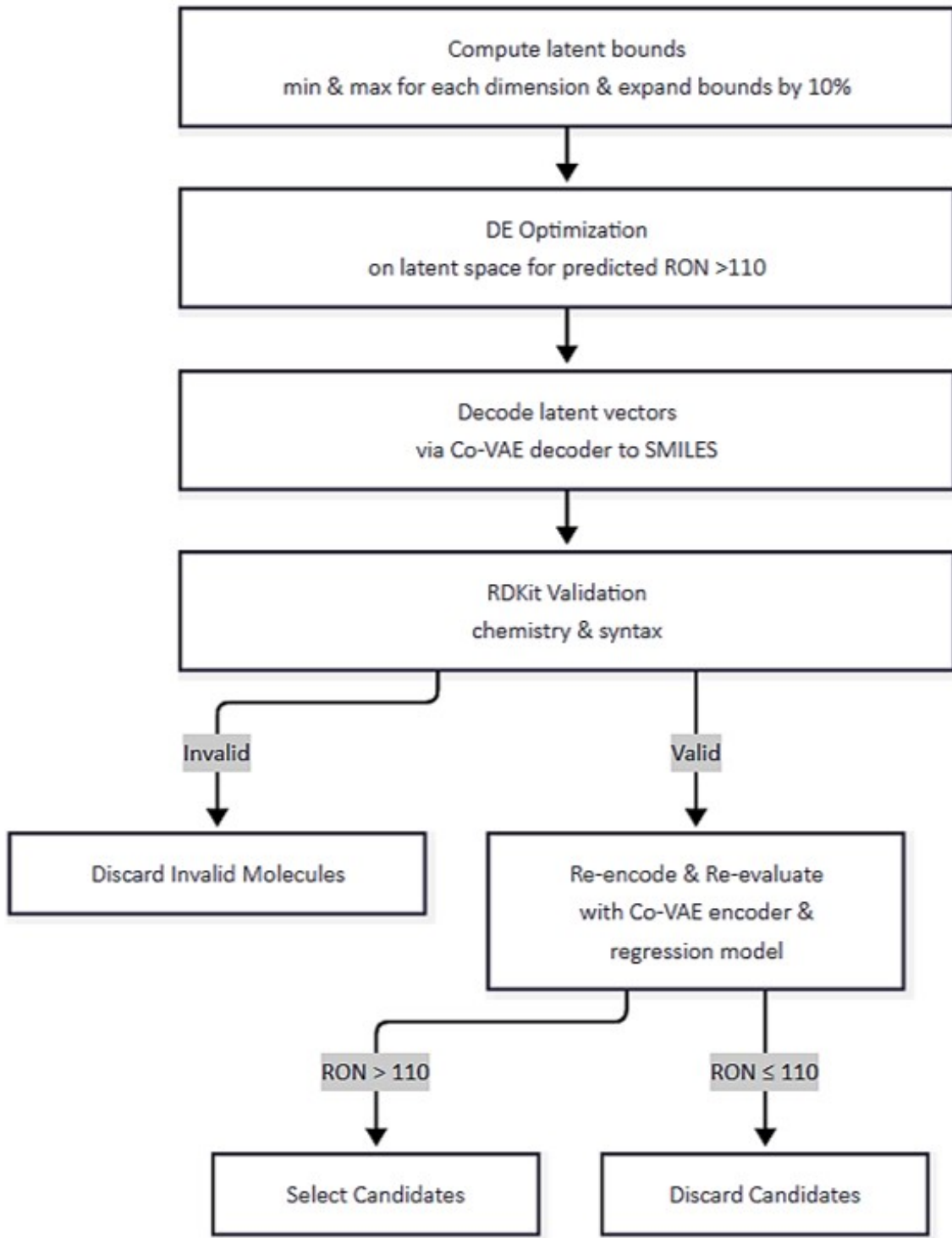


Figure 5: Workflow for the generative fuel design using Co-VAE and regression models.

that fail this test. Beyond this initial screening, each decoded molecule was re-encoded using the Co-VAE encoder and re-evaluated with the regression model to confirm if its predicted RON remains above 110. This extra validation is essential because the VAE generates latent representations by sampling from a distribution, meaning the latent vector passed to the decoder is effectively a perturbed version of its ideal representation. Such perturbations can lead to fluctuations in the predicted RON, even if the molecule is chemically sound. This inherent variability—central to the variational approach—broadens chemical space exploration and necessitates a dual screening process to ensure robust, high-performance fuel candidates. This robust validation framework filters out decoding artifacts, ensuring that only reliable, high-performance fuel candidates progress to further experimental evaluation. The complete workflow for the fuel molecule generation is shown in Figure 5.

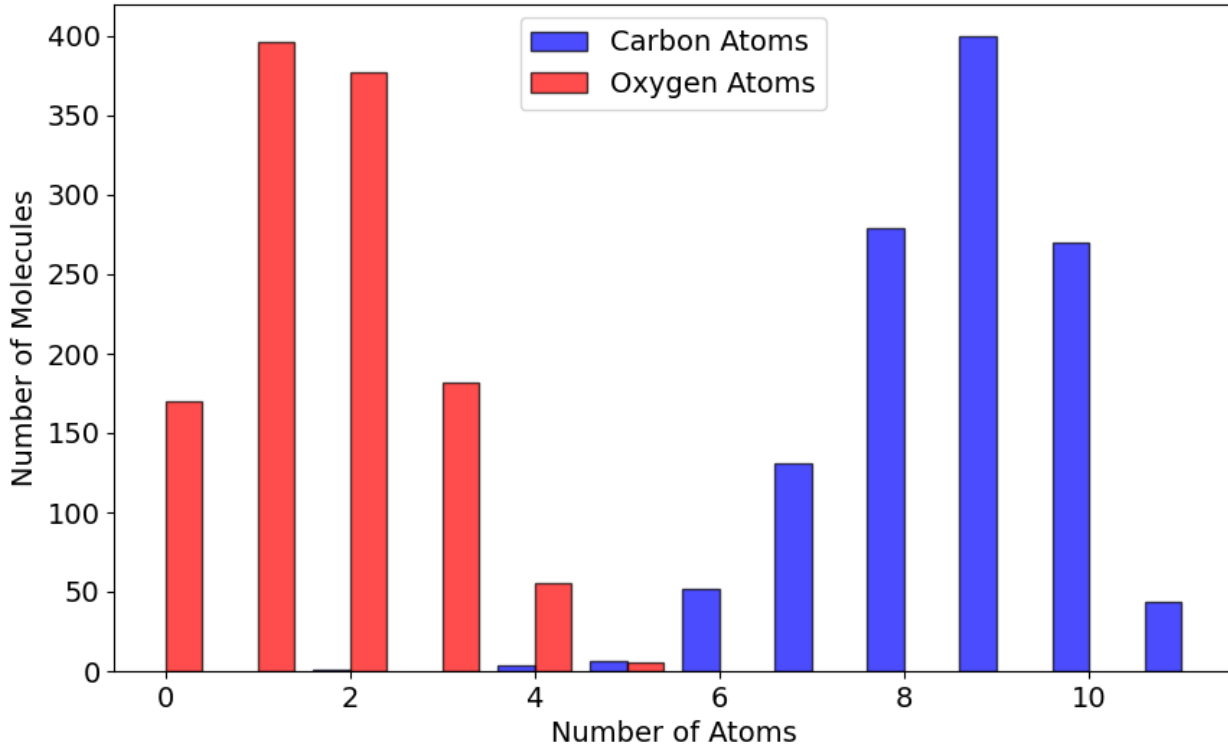


Figure 6: Distribution of carbon and oxygen atoms in the unique generated molecules.

The combination of DE search, Co-VAE decoding, and two-step screening yielded a set of 1189 unique and valid SMILES with predicted RON values exceeding the threshold of

110. These represent 1185 unique chemical species. Among the 1185 species, 264 are already present in the Co-VAE training set; of these, two are included in the RON regression training dataset. Therefore, the process generated 921 unique species that the Co-VAE model had not seen. It is essential to note that these molecules were obtained from a single instance of the latent-space screening procedure. Due to the stochastic nature of the DE algorithm, which is sensitive not only to initial starting conditions and prone to local convergence but also to the number of iterations and the chosen population size, both of which influence the width and depth of the search, the candidate sets obtained can vary between different optimization runs. While a more exhaustive exploration of the latent space might uncover an even broader array of high-performance fuel molecules, such a comprehensive search is out of the scope of this work and will be pursued in future studies. As illustrated in Figure 6, the generated molecules present a wide range of carbon and oxygen atom counts, highlighting the elemental diversity among the high-RON candidates. Furthermore, Figure 7 shows a sample set of generated molecules exhibiting $\text{RON} > 110$, which predominantly features branched structures, alcohols, ethers, and aldehydes—functional groups known to enhance RON. This sample set not only reflects the depth of the current methodology for exploration of the latent space but also demonstrates the effectiveness of the screening strategy, revealing the diversity inherent in the search process for high-performance fuel molecules.

Conclusions

In this study, a co-optimized Variational Autoencoder (Co-VAE) framework was developed and tailored explicitly for fuel molecular design, aiming to predict and enhance the Research Octane Number (RON). Integrating a property prediction component directly into the generative model, the latent space was steered to capture features relevant to molecular reconstruction and property estimation. Through rigorous hyperparameter optimization using Bayesian optimization, the Co-VAE architecture was fine-tuned to maximize reconstruction

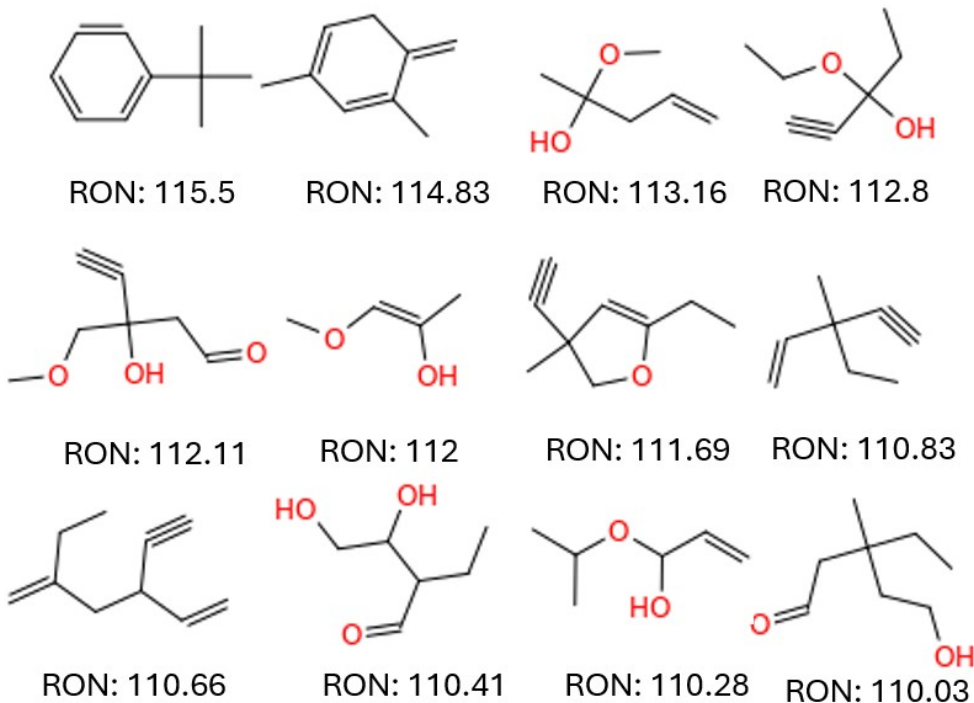


Figure 7: A sample set of generated molecules with RON > 110.

accuracy, validity of generated molecules, and RON prediction capability. Leveraging latent space embeddings, a regression model was subsequently developed to further improve the accuracy of RON predictions. Utilizing differential evolution within the learned latent space, chemically valid novel molecules were screened with predicted RON values exceeding 110, demonstrating the efficacy of our integrated generative and predictive modeling approach.

This framework can help identify promising fuel molecules by directing the search toward property-optimized regions of the latent space, reducing the need to randomly sample large chemical databases. The identified high-RON candidates provide a valuable starting point for further exploration. Future studies can extend this screening process by evaluating additional critical fuel properties such as energy density, volatility, and emission profiles. Incorporating these properties into the predictive model would enable a more comprehensive assessment of fuel viability, ensuring that selected molecules meet multiple performance criteria. Additionally, integrating environmental and economic considerations, such as synthesizability, cost, and other constraints (e.g., toxicity, stability, etc.) could further refine

the selection process, ultimately identifying practical and sustainable fuel solutions.

To enhance and expand the proposed methodology, future work will focus on fine-tuning the downselection process of the GDB-13 database to curate a dataset enriched with fuel-like species, potentially improving the relevance and applicability of the generated molecules. Leveraging transfer learning techniques, the Co-VAE can be initially trained on an extensive database with abundant property data before being fine-tuned for the RON prediction task, benefiting from the broader chemical knowledge while specializing in fuel properties. Implementing multi-task learning approaches, which simultaneously predict multiple properties within the regression model, can capture interrelated property trends and enhance overall predictive performance. Furthermore, by embedding UQ methods,⁹ the model could not only flag candidates with high predictive confidence—ideal for selection and experimental validation—but also identify regions of the latent space with higher uncertainty. These uncertain compounds can guide further data collection and model refinement, ensuring that exploration focuses on promising and underrepresented chemical spaces. Such an approach would refine the screening process, evolving the framework into a more robust and versatile tool for advanced fuel design, thereby contributing to the development of cleaner and more efficient energy sources. In addition, it is noted that standard methods for measuring RON, have experimental repeatability ranges of approximately ± 1 RON. The data-driven approach currently exceeds this threshold, reinforcing the need for larger and more diverse datasets to reduce predictive uncertainty. Lastly, extending this framework to multi-component blends constitutes an important next step, as real engines commonly operate with complex fuel mixtures exhibiting non-linear synergistic effects.

Acknowledgement

The submitted manuscript has been created by UChicago Argonne, LLC, Operator of Argonne National Laboratory (Argonne). The U.S. Government retains for itself, and others

acting on its behalf, a paid-up nonexclusive, irrevocable worldwide license in the said article to reproduce, prepare derivative works, distribute copies to the public, and perform publicly and display publicly, by or on behalf of the Government. This work was supported by the U.S. Department of Energy (DOE), Office of Science under contract DE-AC02-06CH11357. GPU computing resources from Argonne's Laboratory Computing Resource Center (LCRC) cluster Swing and Leadership Computing Facility (ALCF) supercomputer Polaris were used for this study. The authors would like to acknowledge funding support from Aramco Americas – Detroit for this work.

References

- (1) Romanelli, V.; Annunziata, D.; Cerchia, C.; Cerciello, D.; Piccialli, F.; Lavecchia, A. Enhancing De Novo Drug Design across Multiple Therapeutic Targets with CVAE Generative Models. *ACS Omega* **2024**, *9*, 43963–76.
- (2) Dollar, O.; Joshi, N.; Beck, D. A.; Pfaendtner, J. Attention-based generative models for de novo molecular design. *Chem Sci* **2021**, *12*, 8362–72.
- (3) Wang, S.; Lin, T.; Peng, T.; Xing, E.; Chen, S.; Kara, L. B.; Cheng, X. TopMT-GAN: a 3D topology-driven generative model for efficient and diverse structure-based ligand design. *Chem Sci* **2025**, *16*, 2796–809.
- (4) Dodds, M.; Guo, J.; Löhr, T.; Tibo, A.; Engkvist, O.; Janet, J. P. Sample efficient reinforcement learning with active learning for molecular design. *Chem Sci* **2024**, *15*, 4146–60.
- (5) Liu, Y.; Liu, R.; Duan, J.; Wang, L.; Zhang, X.; Li, G. Deep generative fuel design in low data regimes via multi-objective imitation. *Chem Eng Sci* **2023**, *274*, 118686.
- (6) Rittig, J. G.; Ritzert, M.; Schweidtmann, A. M.; Winkler, S.; Weber, J. M.; Morsch, P.;

others. Graph machine learning for design of high-octane fuels. *AIChE J* **2023**, *69*, e17971.

(7) Anufriev, S.; Hellier, P.; Ladommatos, N. Generation of Novel Fuels Optimized for High-Knock Resistance with a Long Short-Term Memory Model. *Energy & Fuels* **2025**, *39*, 13044–13053.

(8) Kuzhagaliyeva, N.; Horváth, S.; Williams, J.; Nicolle, A.; Sarathy, S. M. Artificial intelligence-driven design of fuel mixtures. *Commun Chem* **2022**, *5*, 111.

(9) Yalamanchi, K. K.; Kommalapati, S.; Pal, P.; Kuzhagaliyeva, N.; AlRamadan, A. S.; Mohan, B.; others. Uncertainty quantification of a deep learning fuel property prediction model. *Appl Energy Combust Sci* **2023**, *16*, 100211.

(10) vom Lehn, F.; Brosius, B.; Broda, R.; Cai, L.; Pitsch, H. Using machine learning with target-specific feature sets for structure–property relationship modeling of octane numbers and octane sensitivity. *Fuel* **2020**, *281*, 118772.

(11) SubLaban, A.; Kessler, T. J.; Van Dam, N.; Mack, J. H. Artificial neural network models for octane number and octane sensitivity: a quantitative structure property relationship approach to fuel design. *J Energy Resour Technol* **2023**, *145*, 102302.

(12) Mohan, B.; Chang, J. Chemical SuperLearner (ChemSL)-An automated machine learning framework for building physical and chemical properties model. *Chem Eng Sci* **2024**, *294*, 120111.

(13) Chen, Z.; vom Lehn, F.; Pitsch, H.; Cai, L. Design of novel high-performance fuels with artificial intelligence: Case study for spark-ignition engine applications. *Applications in Energy and Combustion Science* **2025**, *23*, 100341.

(14) Liu, R.; Liu, R.; Liu, Y.; Wang, L.; Zhang, X.; Li, G. Design of fuel molecules based on variational autoencoder. *Fuel* **2022**, *316*, 123426.

(15) Yalamanchi, K. K.; Pal, P.; Mohan, B.; AlRamadan, A. S.; Badra, J. A.; Pei, Y. A Variational Autoencoder Model Toward Molecular Structure Representation Learning of Fuels. *J. Energy Res. Technol. Part A* **2025**, *1*, 052301.

(16) Fu, H.; Li, C.; Liu, X.; Gao, J.; Celikyilmaz, A.; Carin, L. Cyclical annealing schedule: A simple approach to mitigating kl vanishing. *arXiv* **2019**, arXiv:1903.10145.

(17) Klushyn, A.; Chen, N.; Kurle, R.; Cseke, B.; van der Smagt, P. Learning Hierarchical Priors in VAEs. *NeurIPS* **2019**, *32*, 2866–75.

(18) Chen, R. T.; Li, X.; Grosse, R. B.; Duvenaud, D. K. Isolating sources of disentanglement in variational autoencoders. *NeurIPS* **2018**, *31*, 2615–25.

(19) Blum, L. C.; Reymond, J. L. 970 million druglike small molecules for virtual screening in the chemical universe database GDB-13. *J Am Chem Soc* **2009**, *131*, 8732–3.

(20) Li, R.; Herreros, J. M.; Tsolakis, A.; Yang, W. Machine learning regression based group contribution method for cetane and octane numbers prediction of pure fuel compounds and mixtures. *Fuel* **2020**, *280*, 118589.

(21) Derfer, J. M.; Board, C. E.; Burk, F. C.; Hess, R. E.; Lovell, W. G.; Randall, R. A.; Sabina, J. R. Knocking Characteristics of Pure Hydrocarbons. 1958; ASTM International, West Conshohocken, PA.

(22) Hochreiter, S.; Schmidhuber, J. Long short-term memory. *Neural Comput* **1997**, *9*, 1735–80.

(23) Nogueira, F. Bayesian Optimization: Open Source Constrained Global Optimization Tool for Python. 2014.

(24) Özair, S.; Pfister, T. TabNet: Attentive Interpretable Tabular Learning. *Proc AAAI Conf Artif Intell* **2021**, *35*.

(25) TabNet GitHub. 2021; Available at: <https://github.com/dreamquark-ai/tabnet> [Accessed: May 2023].

(26) Mohan, B.; Badra, J. A novel automated SuperLearner using a genetic algorithm-based hyperparameter optimization. *Adv Eng Softw* **2023**, *175*, 103358.

(27) Owoyele, O.; Pal, P.; Torreira, A. V.; Probst, D.; Shaxted, M.; Wilde, M.; Senecal, P. K. Application of an automated machine learning-genetic algorithm (AutoML-GA) coupled with computational fluid dynamics simulations for rapid engine design optimization. *Int J Engine Res* **2021**, *23*, 1586–601.

(28) Moiz, A.; Pal, P.; Probst, D.; Pei, Y.; Zhang, Y.; Som, S.; Kodavasal, J. A machine learning-genetic algorithm (ML-GA) approach for rapid optimization using high-performance computing. *SAE Int J Commer Veh* **2018**, *11*, 291–306.

(29) Deb, K.; Pratap, A.; Agarwal, S.; Meyarivan, T. A fast and elitist multiobjective genetic algorithm: NSGA-II. *IEEE Trans Evol Comput* **2002**, *6*, 182–97.

(30) Blank, J.; Deb, K. Pymoo: Multi-objective optimization in python. *IEEE Access* **2020**, *8*, 89497–509.

(31) Virtanen, P.; Gommers, R.; Oliphant, T. E.; Haberland, M.; Reddy, T.; Cournapeau, D.; others. SciPy 1.0: fundamental algorithms for scientific computing in Python. *Nat Methods* **2020**, *17*, 261–72.

(32) Bento, A. P.; Hersey, A.; Flórez, E.; Landrum, G.; Gaulton, A.; Atkinson, F.; others. An open source chemical structure curation pipeline using RDKit. *J Cheminform* **2020**, *12*, 116.